Journal of Magnetism and Magnetic Materials 149 (1995) 53–56

ELSEVIER

Journal of magnetism and magnetic materials

Magnetorheology of ferrofluid composites

J. Popplewell, R.E. Rosensweig *, J.K. Siller

Exxon Research and Engineering Company, Clinton Township, Annandale, NJ 08801, USA

Abstract

Composites consisting of nonmagnetic particles with sizes in the micron range suspended in a ferrofluid constitute an inverse magnetorheological fluid. Structuring occurs in an applied magnetic field and can result in the solidification of the composite. Above a critical level of applied stress the material further transforms to a liquid state. Data confirming the existence of a solidified state are presented based on constant shear rheological measurements. Measurements of the yield stress compare favorably with predictions of theory based on the analysis of unsymmetric stresses in the unyielded, anisotropic medium.

1. Introduction

Viewing a collection of small nonmagnetic spheres in a thin layer of magnetized fluid, Skjeltorp [1] directly observed the crystallization of magnetic 'holes' forming different lattices according to the direction of the field (see Fig. 1). Related structures develop in bulk composites that have been studied in application to magnetoresistivity [2], microwave dichroism [3], and turbulence prevention in fluidized beds [4]. In the present work we study the influence of the structuring on the rheology of a sheared layer of the bulk suspension depicted schematically in Fig. 2. In this context the composite serves as a type of magnetorheological (MR) fluid. In addition to their scientific interest, MR fluids have attracted renewed attention in recent years due to interest in computer-controlled hydraulic systems for vehicles, and other applications [5,6]. The usual MR fluid consists of magnetically susceptible particles with sizes in the micron range suspended in an oil. The inverse MR fluids [7,8], the focus of this study, consist of nonmagnetic particles suspended in a colloidal, magnetizable fluid (ferrofluid).

2. Criterion of chaining

The chaining of magnetized particles depends on the particle volumetric concentration ϕ and the coupling coefficient λ representing the ratio of dipole–dipole interaction to thermal energy [9,10],

$$n = \left[1 - \frac{2}{3}\left(\frac{\phi}{\lambda^2}\right)e^{2\lambda}\right]^{1/2}, \qquad \lambda = \frac{mM}{24kT}, \tag{1a,b}$$

where n is the mean number of particles in a chain, m the magnetic moment of a particle, M the magnetization of the particle, k the Boltzmann constant, and T the temperature. From (1a), strong chaining indicated by values of $n \gg 1$, occurs at a critical concentration ϕ_c given as

$$\phi_c = \tfrac{3}{2}(\lambda^2/e^{2\lambda}) \tag{2}$$

with the relationship displayed graphically in Fig. 3. For $\phi \geq \phi_c$ the chains can exceed the thickness of a sheared

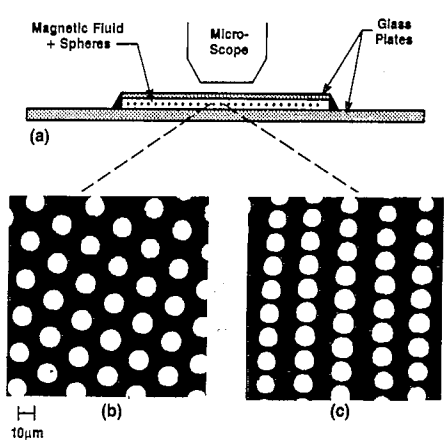

Fig. 1. Alignment of a layer of nonmagnetic spheres in a ferrofluid-induced structure. (a) Experimental arrangement, (b) field normal to layer, (c) field tangential to layer (after Skjeltorp [1]).

* Corresponding author. Fax: +1 (908) 730-3232; email: rerosen@erenj.com.

layer and span the gap between the walls bounding the layer. Ferrofluids stable against magnetic agglomeration and chaining reside in the lower left zone of the diagram, while ordinary MR fluids belong to the upper right zone. The chaining analysis also applies to the effectively diamagnetic interactions between inert particles suspended in ferrofluid. The associated inverse MR composites represent a marriage between magnetic fluid and magnetorheological technologies.

3. Continuum analysis of MR behavior

Recent theory [11] treating MR solid as an anisotropic continuum supporting unsymmetric elastic and magnetic stresses derives a general and exact expression relating the yield stress τ_y of the sheared, unyielded solid to the component of magnetization, $M_\perp$, that is orthogonal to the applied field $\boldsymbol{H}$ having magnitude H.

$$\tau_y = \tfrac{1}{2}\mu_0 M_\perp H, \quad \text{where } M_\perp = |\boldsymbol{M}\cdot(\boldsymbol{I}-\boldsymbol{HH}/H^2)|. \tag{3a,b}$$

The composite containing the ferrofluid is highly anisotropic under the same conditions in which the ferrofluid constituent of the composite is essentially isotropic. Computation [11] from Eq. (3) assuming a model topology of sheared parallel layers, or laminae, results in a relationship for the shear stress τ as a function of the shear angle α. τ versus α exhibits a maximum value, or turning point, that corresponds to the yield condition, with the associated yield stress τ_y given as

$$\frac{\tau_y}{\frac{1}{2}\mu_0 H^2} = \frac{\phi(1-\phi)\chi^2}{2\{(1+\chi)(1+\phi\chi)[1+\chi(1-\phi)]\}^{1/2}}, \tag{4}$$

where $\chi = M/H$ is the susceptibility of the ferrofluid ($M = B/\mu_0 - H$). Predictions of the elastic modulus $G = \tau/\alpha$ for small α using this theory are in good correspondence with values obtained from numerical calculations

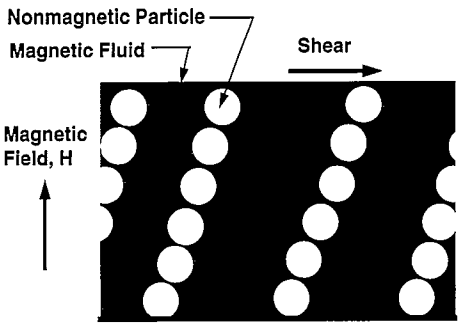

Fig. 2. Schematic illustration of particle chains in a sheared inverse MR fluid. It is likely that the chains tend to coalesce into columns.

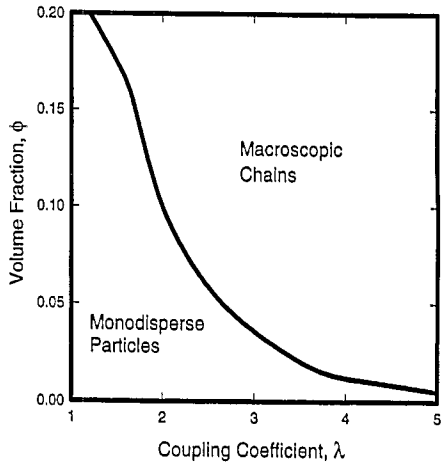

Fig. 3. Phase diagram to illustrate conditions of the liquid/solid transformation of composites.

that treat the interacting particles in a lattice as simple dipoles [11,12]. The dipole behavior should be closely approximated in the inverse MR fluids, whereas MR fluids containing ferrous particles tend to polarize each other at points of contact, thus producing higher-order interactions. Eq. (4) is used below in the comparison of predictions against data for inverse MR fluids.

4. Materials and instrumentation

The nonmagnetic particles of this study are (8 ± 2) μm hollow glass beads of density 1.10 g/cm^3. The ferrofluid is oleic-acid-stabilized, subdomain (~ 9 nm) particles of magnetite dispersed in kerosene carrier. The density of the ferrofluid, 1.18 g/cm^3, nearly matches to that of the beads so that the gravity force plays a nearly negligible role in the structuring. From Eq. (1b), the coupling coefficient for particles of the ferrofluid is $\lambda < 1$, while for the hollow glass spheres of the composite $\lambda = O(10^6)$ at the field intensities used in this study; thus, strong chaining of the hollow glass spheres of the composite is assured. The saturation moment per unit volume of the ferrofluid is $\mu_0 M = 0.045$ T. The susceptibility χ is 1.87, 1.81, 1.47, 1.08, 0.85 and 0.73, at B_0 of 0, 50, 100, 200, 300 and 400×10^{-4} T, respectively. Measurements of rheological properties are made at 24°C with a cone and plate viscometer in which the applied stress is independently controlled; otherwise only the behavior of the yielded composite can be detected. The cone and plate have a diameter of 25 mm with an angle of 0.1 rad between them. The cone apex is separated from the plate by a gap of 0.050 mm, yielding a gap at the outer diameter of 1.30 mm. An aluminum or an iron cone and plate is used; for both materials the surface roughness is 10 μm as determined with a profilometer. A wound field source surrounding the

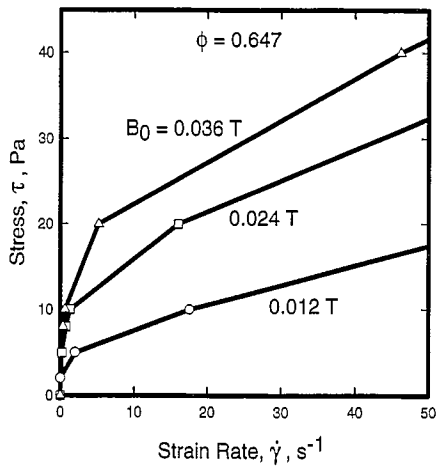

Fig. 4. Experimental rheological curves using a nonmagnetizable cone and plate (aluminum) for an inverse MR fluid with $\phi = 0.647$.

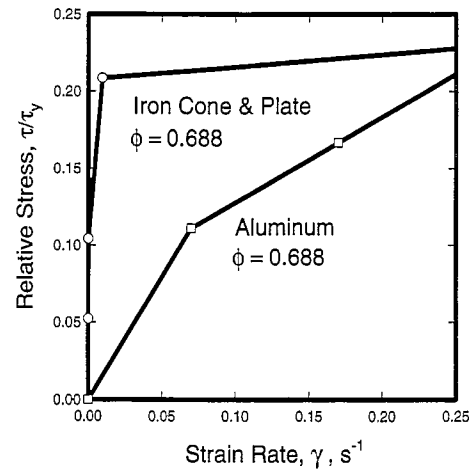

Fig. 6. Rheological data illustrating that the inverse MR fluid sticks to magnetically susceptible walls, and slips at magnetically inert walls. $B_0 = 0.024$ T (aluminum) and 0.028 T (iron).

cone and plate produces a magnetic field oriented normal to the layer of the test fluid.

5. Data

Experimental data for the shear stress τ versus shear rate $\dot{\gamma}$ for inverse MR composites having a ferrofluid volume fraction of $\phi = 0.647$ are shown in Fig. 4. Fig. 5 shows data at various values of ϕ with a constant applied induction $B_0 = 0.036$ T. Any one data curve has the form approximated by the Bingham relationship $\tau = \tau_y + \eta'\dot{\gamma}$, where η' is known as the plastic viscosity, $\dot{\gamma}$ is the shear rate, and τ_y corresponds to the straight-line extrapolation of the high shear portion of the data to the strain axis (dynamic yield stress). Maximum values of $\dot{\gamma}$ ranged from 300 to 400 s^{-1}. The rounded shapes of the curves might result from wall slippage and so the question arises – can a true state of unyielded solid exist up to a sharp value of transitional stress? Fig. 6 presents data on a 200 to 1 expanded scale of strain rate to examine this issue more clearly; the rheometer instrumentation permits this precision. It can be inferred that for the nonmagnetizable (aluminum) cone and plate a detectable rate of cone rotation is established at any measured small rate of strain. If the layer experiences homogeneous deformation then it follows that the yield stress is absent. An alternative interpretation is that slip occurs at the wall, i.e. that deformation is inhomogeneous across the layer. In that case, due to the image forces that arise [13], the same sample placed in the gap between a magnetizable (iron) cone and plate should tend to stick to the walls, and wall slip should be prevented over some finite range of applied stresses. Reference to the magnetizable (iron) cone and plate data curve in Fig. 6 nicely supports the no-slip expectation as the sample exhibits sensibly infinitesimal deformation rates up to a finite value of the applied stress (static yield stress). Additional measurements show that the dynamic yield stress is essentially the same, independent of the equally rough (aluminum or iron) materials making up the cone and plate.

In view of the above it seems compelling that if wall slip could be prevented under all operating conditions then the measured curves would most closely follow the idealized Bingham form with static yield stress approaching the dynamic yield stress value. It is on that assumption that the theory for yield stress [11] was developed and, in Section 6, the data are compared against the theory imputing the experimental values of dynamic yield stress as the asymptotic value of static yield stress.

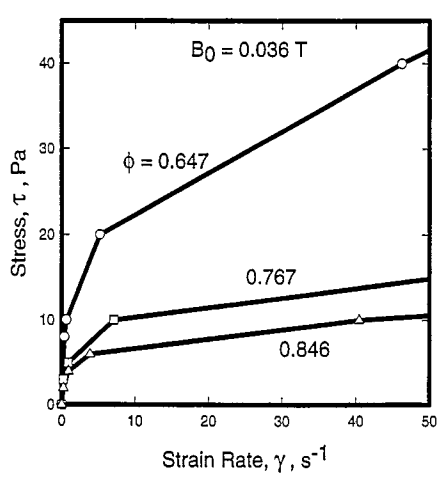

Fig. 5. Experimental rheological curves using a nonmagnetizable cone and plate for inverse MR fluids with a constant applied induction of $B_0 = 0.036$ T.

6. Predictions compared to data

The solid lines in Fig. 7 represent theoretical values of the normalized yield stress versus the volume fraction of magnetic fluid in the composite for different constant values of susceptibility. At the extremes ($\phi = 0$ or 1) the yield stress disappears as the material is then isotropic, and so a maximum exists in between. Values of loading to the left of the maximum are most readily accessible for MR fluids, in which case ϕ represents the volume fraction of magnetizable particles, whereas values to the right apply to realizable inverse MR fluids. The data points shown in Fig. 7 represent normalized dynamic yield stress values derived from the data of Figs. 4 and 5. A small correction, the chord susceptibility $\overline{\chi} = \chi(H \sec \theta)$, where $\theta = \pi/4$, rather than $\chi(H)$, is used to improve the accordance with the field distribution along principal axes in the deformed sample. The agreement of theory and measurement in Fig. 7 is very good over this limited set of data; more data are needed to determine whether this trend will persist.

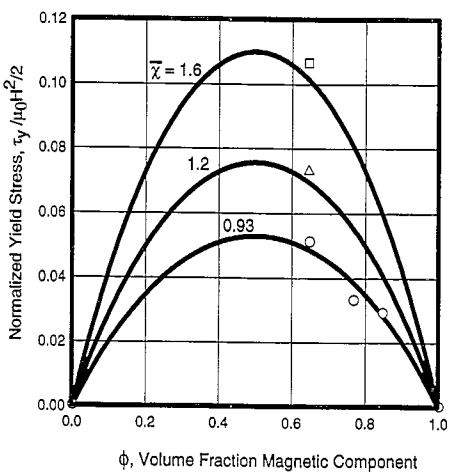

Fig. 7. Theoretical predictions of the yield stress compared with the experimental data of this study.

7. Conclusions

Ferrofluid composites can transform to a solid in a magnetic field, and then transform again to a fluid state when the applied shear stress exceeds a critical value. Continuum analysis assuming no slip at the walls predicts the nonlinear dependence of the yield stress on loading over the entire range of compositions. Measurements using constant values of applied stress clarify the nature of the yield stress in the inverse MR systems. Measured values of dynamic yield stress compare favorably with the theoretical predictions based on a model geometry of laminae which undoubtedly only crudely resembles the chain and column structures thought to be present in the inverse MR samples; the predictions appear to be insensitive to this variance.

References

[1] A.T. Skjeltorp, Phys. Rev. Lett. 51 (1983) 2306; J. Appl. Phys. 57 (1985) 3285.
[2] A.S. Kent and D. Midgley, Electron. Lett. 20 (1984) 960.
[3] J. Popplewell, P. Davies, J.P. Llewellyn and K. O'Grady, J. Magn. Magn. Mater. 65 (1987) 235.
[4] R.E. Rosensweig and G. Ciprios, Powder Technol. 64 (1991) 115.
[5] A. Pinkos, E. Shtarkman and T. Fitzgerald, Automotive Eng. 101 (1993) 19.
[6] J.D. Carlson and K.D. Weiss, Machine Design, August 8 (1994) 61.
[7] B.E. Kashevskii, V.I. Kordonskii and I.V. Prokhorov, Magnetohydrodynamics 3 (1988) 368 (Plenum, New York).
[8] E. Lemaire and G. Bossis, J. Rheol. 35 (1991) 1345.
[9] P.G. deGennes and P. Pincus, Phys. Kondens. Mater. 11 (1970) 189.
[10] A.P. Gast and C.F. Zukowski, Adv. Colloidal Interfacial Sci. 30 (1989) 153.
[11] R.E. Rosensweig, J. Rheol. 39 (1995) 179.
[12] L.C. Davis, Appl. Phys. Lett. 60 (1992) 319.
[13] J.D. Jackson, Classical Electrodynamics, 2nd edn. (Wiley, New York, 1975), p. 147.